

Two-proton radioactivity within a Coulomb and proximity potential model for deformed nuclei

K. P. Santhosh **Department of Physics, University of Calicut, Kerala 673635, India**and School of Pure and Applied Physics, Kannur University, Swami Anandatheertha Campus, Payyanur 670327, Kerala, India*

(Received 8 October 2022; accepted 26 October 2022; published 15 November 2022)

The half-lives of two-proton ($2p$) emitters ${}^6\text{Be}$, ${}^{12}\text{O}$, ${}^{16}\text{Ne}$, ${}^{19}\text{Mg}$, ${}^{45}\text{Fe}$, ${}^{48}\text{Ni}$, ${}^{54}\text{Zn}$, and ${}^{67}\text{Kr}$ have been predicted using the Coulomb and proximity potential model for deformed nuclei (CPPMDN) incorporating ground-state deformation (β_2) and orientation effect, and the predicted values are compared with experimental data. As predicted values are in agreement with experimental data I extended my studies to 51 nuclei, whose decay are energetically possible with released energy $Q_{2p} > 0$ for which $2p$ radioactivity is not yet experimentally detected, and the predicted half-life values are compared with other theoretical models/formulas. I hope the future experimental investigations will be guided by these predictions. The new Geiger Nuttall plot connecting $\log_{10}[T_{1/2}(s)]$ computed using the CPPMDN versus $[Z_d^{0.8} + \ell^\beta]Q_{2p}^{-1/2}$ is found to be linear which shows the reliability of my calculations. It is found for the first time that $2p$ radioactivity also obeys the linear nature of a universal curve connecting $\log_{10}[T_{1/2}(s)]$ versus $-\ln P$ as that of the proton, α , and cluster radioactivity.

DOI: [10.1103/PhysRevC.106.054604](https://doi.org/10.1103/PhysRevC.106.054604)

I. INTRODUCTION

The simultaneous emission of two protons from an exotic nucleus near or beyond the proton drip line is known as two-proton ($2p$) radioactivity. This phenomenon was first predicted by Zel'dovich [1] and independently by Goldansky [2,3] in 1960. The two-proton emission was experimentally observed, only four decades after its first prediction. The development of advanced detection technologies and radioactive beam facilities led to the detection of true $2p$ radioactivity ($Q_{2p} > 0$ and $Q_{1p} < 0$, where Q_{2p} and Q_{1p} are the energy released in $2p$ and $1p$ radioactivity, respectively) from ${}^{45}\text{Fe}$ at GSI [4] and at GANIL [5]. Later $2p$ radioactivity was detected from the nuclei ${}^{54}\text{Zn}$ [6], ${}^{48}\text{Ni}$ [7], ${}^{19}\text{Mg}$ [8], ${}^{67}\text{Kr}$ [9], and the extremely short-lived $2p$ radioactivity from ground state was also reported from ${}^6\text{Be}$ [10], ${}^{12}\text{O}$ [11], and ${}^{16}\text{Ne}$ [11].

A systematic theoretical investigation on $2p$ radioactivity as a three-body problem was performed by Swan [12] in 1965. Also many theoretical studies have been performed using a relativistic mean-field plus state-dependent BCS approach [13–18] and a macroscopic-microscopic approach with the Nilsson-Strutinsky prescription [19,20]. The $2p$ radioactivity can be classified into three types: (1) as a three-body emission, (2) sequential emission, and (3) as a ${}^2\text{He}$ cluster emission. In three-body emission [21–24], the nuclear core and the two protons separate simultaneously, and the two protons are only relevant to the final correlation and emitted from the parent nucleus. In the sequential emission [2,25], the initial nucleus first decays to an intermediate state by emitting a proton,

and then the intermediate state decays by emitting another proton. In ${}^2\text{He}$ cluster emission the strongly correlated two protons constitute a quasibound state and after penetrating through the barrier it separates into two protons. This category includes the effective liquid drop model (ELDM) [26], the Gamow-like model (GLM) [27], the generalized liquid drop model (GLDM) [28], etc. Further four parameter empirical formula (EF) by Sreeja and Balasubramaniam [29] and the two-parameter new Geiger Nuttall law (GNL) by Liu *et al.*, [30] were proposed.

The Coulomb and proximity potential model for deformed nuclei (CPPMDN) [31,32] was introduced to study α and cluster radioactivity, which is an improved version of Coulomb and proximity potential model (CPPM) [33,34], including ground-state deformation and orientation effects. Using the CPPMDN, $2p$ radioactivity of several even- Z nuclei have been studied [35] and found that inclusion of deformation reduces the half-life and the predicted values are close to the experimental values with least standard deviation, $\sigma = 1.03$. Most of the two-proton emitters considered in the paper are deformed and in some cases (e.g., ${}^{67}\text{Kr}$) both shape and structure change occur. The studies presented in Refs. [35,36] show that the lifetime of ${}^{67}\text{Kr}$ dramatically reduces as the deformation and structure changes.

In this paper I first calculate half-lives of $2p$ radioactivity using the CPPMDN for experimentally known nuclei, and the predicted values are compared with experimental data and other theoretical models/formulas. Then I extended my studies to other 51 nuclei for which $2p$ radioactivity is not yet experimentally detected. Section I of this paper deals with the Introduction, Sec. II gives the methodology used for the paper, Sec. III gives the results and discussion, and Sec. IV gives the conclusion of the entire paper.

* drkpsanthosh@gmail.com

II. THE METHODOLOGY

A. The model CPPMDN

In the CPPMDN the sum of the Coulomb potential for deformed nuclei $V_C(r, \theta)$, the two-term proximity potential for deformed nuclei $V_{P2}(r, \theta)$, and the centrifugal potential are taken as the interacting potential for the postscission region. It is given by

$$V = V_C(r, \theta) + V_{P2}(r, \theta) + \frac{\hbar^2 \ell(\ell + 1)}{2\mu r^2}, \quad (1)$$

where ℓ represents the angular momentum and μ is the reduced mass.

The Coulomb potential for two deformed and oriented nuclei with higher multipole deformations [37,38] is taken from Ref. [39] and is given as

$$V_C(r, \theta) = \frac{Z_1 Z_2 e^2}{r} + 3Z_1 Z_2 e^2 \sum_{\lambda, i=1,2} \frac{1}{2\lambda + 1} \frac{R_{0i}^\lambda}{r^{\lambda+1}} Y_\lambda^{(0)}(\alpha_i) \times \left[\beta_{\lambda i} + \frac{4}{7} \beta_{\lambda i}^2 Y_\lambda^{(0)}(\alpha_i) \delta_{\lambda,2} \right]. \quad (2)$$

Here $r = z + C_1 + C_2$ is the distance between the fragment centers. C_1 and C_2 are the Süssmann central radii of fragments,

$$R_i(\alpha_i) = R_{0i} \left[1 + \sum_{\lambda} \beta_{\lambda i} Y_\lambda^{(0)}(\alpha_i) \right], \quad (3)$$

where $R_{0i} = 1.28A_i^{1/3} - 0.76 + 0.8A_i^{-1/3}$. Here α_i is the angle between the radius vector and the symmetry axis of the i th nuclei, and it is to be noted that the quadrupole interaction term proportional to $\beta_{21}\beta_{22}$ is neglected because of its short-range character.

The two-term proximity potential for the interaction between a deformed and a spherical nucleus [40] given as

$$V_{P2}(r, \theta) = 2\pi \left[\frac{R_1(\alpha)R_C}{R_1(\alpha) + R_C + S} \right]^{1/2} \left[\frac{R_2(\alpha)R_C}{R_2(\alpha) + R_C + S} \right]^{1/2} \times \left[\left[\varepsilon_0(S) + \frac{R_1(\alpha) + R_C}{2R_1(\alpha)R_C} \varepsilon_1(S) \right] \times \left[\varepsilon_0(S) + \frac{R_2(\alpha) + R_C}{2R_2(\alpha)R_C} \varepsilon_1(S) \right] \right]^{1/2}, \quad (4)$$

where $R_1(\alpha)$ and $R_2(\alpha)$ are the principal radii of curvature of the daughter nuclei where the polar angle is α , R_C is the radius of the spherical cluster, S is the distance between the surfaces along the straight line connecting the fragments, and $\varepsilon_0(S)$ and $\varepsilon_1(S)$ are the one-dimensional slab-on-slab function. The relation between α and θ in Eqs. (3) and (4) is given by the equation (see Fig. 5 of Ref. [40]),

$$\frac{\cos(\theta - \alpha)}{R_T(\alpha)} + \frac{\sin(\theta - \alpha)}{R'_T(\alpha)} = \frac{1}{R}, \quad (5)$$

where $R_T(\alpha)$ is the radius of deformed nuclei in a direction α from the symmetry axis, $R'_T(\alpha) = (dR/d\alpha)$ and R is the distance between the fragment centers,

$$V = a_0(L - L_0)^n \quad (6)$$

is the simple power-law interpolation [41] used for the internal part or precession (overlap) region of the barrier. Here $L = z + 2C_1 + 2C_2$ is the overall separation of the fragments and $L_0 = 2C$ is the diameter of the parent nuclei with C as the Süssmann central radii of the parent nuclei. By equating the two potentials at the touching point the value of the constants a_0 and n can be determined.

The penetrability P through the barrier is given by

$$P = \exp \left\{ -\frac{2}{\hbar} \int_a^b \sqrt{2\mu(V - Q)} dz \right\}. \quad (7)$$

Here μ is the reduced mass. The equation $V(a) = V(b) = Q$ provides the condition to determine the turning points “ a ” and “ b ”, and Q is the energy released.

The barrier penetrability P of a cluster in a deformed nucleus is different in different directions. The averaging of penetrability over different directions is performed using the equation,

$$P = \frac{1}{2} \int_0^\pi P(Q, \theta, \ell) \sin(\theta) d\theta, \quad (8)$$

where $P(Q, \theta, \ell)$ is the penetrability of a cluster in direction θ from the symmetry axis for axially symmetric deformed nuclei.

The decay half-life is given by

$$T_{1/2} = \left(\frac{\ln 2}{\nu P} \right). \quad (9)$$

Here the assault frequency is $\nu = (\frac{2E_v}{\hbar})$. The empirical vibration energy E_v is given as [42]

$$E_v = \frac{\pi \hbar (2Q/\mu)^{1/2}}{2(C_1 + C_2)}. \quad (10)$$

Here Q is the released energy, μ is the reduced mass; and C_1 and C_2 are the Süssmann central radii of the fragments.

In the case of spherical nuclei, (in the CPPM), the interacting barrier is given by

$$V = \frac{Z_1 Z_2 e^2}{r} + V_p(z) + \frac{\hbar^2 \ell(\ell + 1)}{2\mu r^2} \quad \text{for } z > 0, \quad (11)$$

where “ z ” is the distance between the near surfaces of the fragments. V_p is the proximity potential [43] given as

$$V_p(z) = 4\pi\gamma b \left[\frac{C_1 C_2}{(C_1 + C_2)} \right] \Phi \left(\frac{z}{b} \right), \quad (12)$$

with γ as the nuclear surface tension coefficient, and Φ as the universal proximity potential [43].

Then the penetrability and half-lives can be determined using Eqs. (7) and (9).

B. EF and GNL

The EF of Sreeja and Balasubramaniam [29] is given as

$$\log_{10}[T_{1/2}(s)] = (a_1 \ell + b_1) \xi + (c_1 \ell) + d_1, \quad (13)$$

where $\xi = Z_d^{0.8} Q_{2p}^{-1/2}$, Z_d being the charge of the daughter nucleus and the constants are given as $a_1 = 0.1578$, $b_1 = 1.9474$, $c_1 = -1.8795$, and $d_1 = -24.847$.

TABLE I. Comparison of our predicted half-lives for $2p$ radioactivity from various nuclei with experimental data and other theoretical models and/or formulas. The GLDM values are taken from Ref. [46]. Q values are computed using mass tables of Wang *et al.* [47].

Nuclei	Q_{2p} (MeV)	$\log_{10}[T_{1/2}(s)]$				
		Expt.	Present	GLDM	GNL	EF
${}^6_4\text{Be} \rightarrow {}^4_2\text{He} + 2p$	1.372	-20.30	-21.98		-23.81	-21.95
${}^{12}_8\text{O} \rightarrow {}^{10}_6\text{C} + 2p$	1.737	-21.10	-21.08		-20.37	-18.65
${}^{16}_{10}\text{Ne} \rightarrow {}^{14}_8\text{O} + 2p$	1.403	-20.38	-18.26		-17.78	-16.17
${}^{19}_{12}\text{Mg} \rightarrow {}^{17}_{10}\text{Ne} + 2p$	0.763	-11.40	-12.22		-12.15	-10.78
${}^{45}_{26}\text{Fe} \rightarrow {}^{43}_{24}\text{Cr} + 2p$	1.190 ^a	-2.42	-2.86	-3.28	-3.16	-2.16
${}^{48}_{28}\text{Ni} \rightarrow {}^{46}_{26}\text{Fe} + 2p$	1.950 ^a	-2.08	-7.32	-7.73	-7.11	-5.95
${}^{54}_{30}\text{Zn} \rightarrow {}^{52}_{28}\text{Ni} + 2p$	1.650 ^a	-2.43	-3.39	-4.40	-4.08	-3.05
${}^{67}_{36}\text{Kr} \rightarrow {}^{65}_{34}\text{Se} + 2p$	1.520 ^a	-1.70	0.98	-0.46	0.85	1.68

^a Q values are taken from Ref. [46].

The GNL of Liu *et al.* [30] is given as

$$\log_{10}[T_{1/2}(s)] = a_2[Z_d^{0.8} + \ell^\beta]Q_{2p}^{-1/2} + b_2. \quad (14)$$

Here β reflects the effect of angular momentum on $2p$ radioactivity, and its value is $\beta = 0.25$. The constants of the formula are given as $a_2 = 2.032$ and $b_2 = -26.832$.

III. RESULTS AND DISCUSSION

The energy released in $2p$ radioactivity Q_{2p} is given by

$$Q_{2p} = \Delta M_P - (\Delta M_{2p} + \Delta M_d) + k(Z_p^\varepsilon - Z_d^\varepsilon). \quad (15)$$

Here ΔM_P , ΔM_{2p} , and ΔM_d are the mass excess of parent nuclei, $2p$ system, and daughter nuclei, respectively. The mass excess of the $2p$ system is equal to twice the mass excess of a proton, i.e., $\Delta M_{2p} = 2\Delta M_p$ since $2p$ system is an unbound system consisting of two protons. The electron screening effect on the energy of emitted two protons is included by using the term $k(Z_p^\varepsilon - Z_d^\varepsilon)$. The term kZ^ε is the total binding energy of Z electrons in the atom. For nuclei with $Z \geq 60$, $k = 8.7$ eV, and $\varepsilon = 2.517$; for nuclei with $Z < 60$, $k = 13.6$ eV, and $\varepsilon = 2.408$ [44,45]. The Q_{2p} value must be positive for the $2p$ decay to occur.

Table I gives the predicted half-lives for $2p$ radioactivity from various nuclei ${}^6\text{Be}$, ${}^{12}\text{O}$, ${}^{16}\text{Ne}$, ${}^{19}\text{Mg}$, ${}^{45}\text{Fe}$, ${}^{48}\text{Ni}$, ${}^{54}\text{Zn}$, and ${}^{67}\text{Kr}$ using the CPPMDN and their comparison with the experimental data and other theoretical models and/or formulas. It should be noted that the nuclei ${}^6\text{Be}$, ${}^{19}\text{Mg}$, and ${}^{45}\text{Fe}$ are true $2p$ radioactive ($Q_{2p} > 0$, $Q_{1p} < 0$) nuclei on the other hand ${}^{12}\text{O}$, ${}^{16}\text{Ne}$, ${}^{48}\text{Ni}$, ${}^{54}\text{Zn}$, and ${}^{67}\text{Kr}$ are the not true $2p$ radioactive ($Q_{2p} > 0$, $Q_{1p} > 0$) nuclei. The first column represents the reaction, the second column gives the released energy Q_{2p} in MeV. The third–seventh columns represent the experimental logarithm of half-lives, the predictions of the present paper, the predictions of Wang *et al.* [46] using GLDM, values computed using the GNL [30], and that computed using the EF [29], respectively. The Q_{2p} values are computed using mass excess taken from recent tables of Wang *et al.* [47] and as the computed Q_{2p} values for ${}^{45}\text{Fe}$, ${}^{48}\text{Ni}$, ${}^{54}\text{Zn}$, and ${}^{67}\text{Kr}$ deviates much from experimental values, Q_{2p} values for these nuclei are taken from Ref. [46] in which the values are computed using mass excess taken from the table Koura *et al.* [48]. In the present paper for the computation of half-lives the ground-state quadrupole deformation (β_2) values are taken from the recent table Finite-range droplet macroscopic

TABLE II. Comparison of our predicted half-lives for various nuclei whose $2p$ radioactivity are energetically possible with other theoretical models and/or formulas. The released energy Q_{2p} and angular momentum ℓ are taken from Ref. [26].

Nuclei	Q_{2p} (MeV)	ℓ	$\log_{10}[T_{1/2}(s)]$						
			Present	ELDM [26]	GLM [27]	SEB [51]	SHF [52]	GNL [30]	EF [29]
${}^{10}_7\text{N}$	1.3	1	-18.02	-17.64	-17.36	-16.76		-18.59	-20.04
${}^{28}_{17}\text{Cl}$	1.965	2	-14.28	-12.95	-13.11	-11.78		-12.46	-14.52
${}^{32}_{19}\text{K}$	2.077	2	-13.66	-12.25	-12.49	-11.13		-11.55	-13.46
${}^{36}_{21}\text{Sc}$	1.993	0	-12.39	-11.74	-12.00	-10.79	-11.12	-11.66	-10.30
${}^{40}_{23}\text{V}$	1.842	0	-10.51	-9.85	-10.15	-8.97	-9.43	-9.73	-8.46
${}^{47}_{27}\text{Co}$	1.042	0	-1.01	-0.11	-0.42	-1.13	-0.97	-0.69	0.21
${}^{52}_{29}\text{Cu}$	0.772	4	8.04	9.36	8.94			8.74	8.62
${}^{56}_{31}\text{Ga}$	2.443	0	-9.40	-8.00	-8.57	-7.41	-7.51	-7.61	-6.42
${}^{57}_{31}\text{Ga}$	2.047	2	-6.59	-5.30	-5.91	-4.94		-4.14	-5.22
${}^{60}_{33}\text{As}$	3.492	4	-10.35	-8.68	-9.40	-7.88		-8.33	-10.84
${}^{61}_{33}\text{As}$	2.282	0	-7.44	-6.12	-6.76	-5.78	-6.07	-5.85	-4.74
${}^{62}_{33}\text{As}$	0.692	2	13.74	14.52	14.06			14.18	13.83

TABLE III. Comparison of our predicted half-lives for various nuclei whose $2p$ radioactivity are energetically possible with other theoretical models and/or formulas. The released energy Q_{2p} and angular momentum ℓ are taken from Ref. [53]. The UFM, GLDM, and ELDM values are taken from Ref. [53].

Nuclei	Q_{2p} (MeV)	ℓ	$\log_{10}[T_{1/2}(s)]$					
			Present	UFM	GLDM	ELDM	GNL	EF
¹⁴ F	0.05	1	12.62	12.22		12.31	25.36	17.93
²² Si	1.58	0	-14.99	-14.61	-18.87	-14.15	-15.03	-13.54
¹⁴ P	1.24	4	-10.24	-8.50	-9.41	-8.44	-10.05	-14.34
²⁴ P	1.24	4	-10.24	-8.50	-9.41	-8.44	-10.05	-14.34
¹⁵ P	1.24	4	-10.24	-8.50	-9.41	-8.44	-10.05	-14.34
²⁶ S	2.36	0	-16.19	-16.09	-19.64	-15.15	-15.91	-14.38
¹⁶ S	2.36	0	-16.19	-16.09	-19.64	-15.15	-15.91	-14.38
²⁸ Cl	2.72	2	-16.35	-15.29	-15.66	-14.49	-14.61	-16.63
¹⁷ Cl	2.72	2	-16.35	-15.29	-15.66	-14.49	-14.61	-16.63
²⁹ Cl	0.10	0	29.62	28.91		29.44	29.25	28.90
¹⁷ Cl	0.10	0	29.62	28.91		29.44	29.25	28.90
³⁰ Ar	3.42	0	-17.35	-17.02	-19.66	-16.15	-16.73	-15.17
¹⁸ Ar	3.42	0	-17.35	-17.02	-19.66	-16.15	-16.73	-15.17
³² K	2.74	2	-15.61	-14.44	-14.78	-13.68	-13.53	-15.42
¹⁹ K	2.74	2	-15.61	-14.44	-14.78	-13.68	-13.53	-15.42
³⁴ Ca	2.51	0	-14.65	-14.46	-14.78	-13.56	-13.88	-12.44
²⁰ Ca	2.51	0	-14.65	-14.46	-14.78	-13.56	-13.88	-12.44
³⁵ Sc	4.98	3	-17.36	-16.10	16.63	-15.57	-16.03	-19.05
²¹ Sc	4.98	3	-17.36	-16.10	16.63	-15.57	-16.03	-19.05
³⁷ Sc	0.38	3	9.72	10.92	10.10	-10.97	12.26	10.92
²¹ Sc	0.38	3	9.72	10.92	10.10	-10.97	12.26	10.92
³⁸ Ti	3.24	0	-15.51	-15.18	-15.38	-14.30	-14.43	-12.96
²² Ti	3.24	0	-15.51	-15.18	-15.38	-14.30	-14.43	-12.96
³⁹ Ti	1.06	0	-5.44	-5.41	-5.55	-4.64	-5.15	-4.07
²² Ti	1.06	0	-5.44	-5.41	-5.55	-4.64	-5.15	-4.07
³⁹ V	4.21	0	-16.74	-16.34	-16.54	-15.49	-15.52	-14.01
²³ V	4.21	0	-16.74	-16.34	-16.54	-15.49	-15.52	-14.01
⁴⁰ V	2.14	0	-11.87	-11.66	-11.80	-10.80	-10.97	-9.64
²³ V	2.14	0	-11.87	-11.66	-11.80	-10.80	-10.97	-9.64
⁴¹ Cr	3.33	0	-14.87	-14.53	-14.72	-13.66	-13.63	-12.19
²⁴ Cr	3.33	0	-14.87	-14.53	-14.72	-13.66	-13.63	-12.19
⁴² Cr	1.48	0	-7.60	-7.40	-7.56	-6.66	-7.03	-5.87
²⁴ Cr	1.48	0	-7.60	-7.40	-7.56	-6.66	-7.03	-5.87
⁴³ Mn	2.48	2	-11.91	-10.65	-11.03	-10.16	-9.45	-10.95
²⁵ Mn	2.48	2	-11.91	-10.65	-11.03	-10.16	-9.45	-10.95
⁴⁴ Mn	0.50	0	9.19	9.80	9.51	10.22	8.47	8.99
²⁵ Mn	0.50	0	9.19	9.80	9.51	10.22	8.47	8.99
⁴⁷ Co	1.02	2	0.11	1.13	0.63	1.37	1.98	0.82
²⁷ Co	1.02	2	0.11	1.13	0.63	1.37	1.98	0.82
⁴⁹ Ni	1.08	0	-0.59	0.23	-0.08	0.67	-0.34	0.55
²⁸ Ni	1.08	0	-0.59	0.23	-0.08	0.67	-0.34	0.55
⁵² Cu	1.13	4	1.54	3.45	2.70	3.34	2.57	1.51
²⁹ Cu	1.13	4	1.54	3.45	2.70	3.34	2.57	1.51
⁵⁵ Zn	0.78	2	7.71	8.77	8.26	8.92	8.99	8.24
³⁰ Zn	0.78	2	7.71	8.77	8.26	8.92	8.99	8.24
⁵⁶ Ga	2.82	0	-11.03	-10.30	-10.83	-9.14	-8.94	-7.70
³¹ Ga	2.82	0	-11.03	-10.30	-10.83	-9.14	-8.94	-7.70
⁵⁷ Ga	1.65	2	-3.73	-3.01	-3.81	-2.20	-1.56	-2.55
³¹ Ga	1.65	2	-3.73	-3.01	-3.81	-2.20	-1.56	-2.55
⁵⁸ Ga	0.51	2	18.27	18.71	17.88	19.33	18.63	18.26
³¹ Ga	0.51	2	18.27	18.71	17.88	19.33	18.63	18.26
⁵⁸ Ge	3.23	0	-12.00	-11.19	-11.73	-10.02	-9.65	-8.38
³² Ge	3.23	0	-12.00	-11.19	-11.73	-10.02	-9.65	-8.38
⁵⁹ Ge	1.60	0	-3.23	-2.73	-3.37	-1.76	-2.42	-1.45
³² Ge	1.60	0	-3.23	-2.73	-3.37	-1.76	-2.42	-1.45
⁶⁰ As	3.32	4	-9.83	-8.37	-9.34	-7.81	-7.86	-10.29
³³ As	3.32	4	-9.83	-8.37	-9.34	-7.81	-7.86	-10.29
⁶¹ As	1.98	0	-5.55	-4.95	-5.61	-3.97	-4.31	-3.26
³³ As	1.98	0	-5.55	-4.95	-5.61	-3.97	-4.31	-3.26
⁶² As	0.59	2	17.51	17.99	17.14	18.58	17.58	17.35
³³ As	0.59	2	17.51	17.99	17.14	18.58	17.58	17.35
⁶³ Se	2.36	0	-7.26	-6.59	-7.22	-5.60	-5.67	-4.56
³⁴ Se	2.36	0	-7.26	-6.59	-7.22	-5.60	-5.67	-4.56
⁶⁴ Se	0.70	0	14.15	14.39	13.69	15.14	12.03	12.39
³⁴ Se	0.70	0	14.15	14.39	13.69	15.14	12.03	12.39
⁶⁵ Br	2.43	2	-6.42	-5.55	-6.37	-4.76	-3.91	-4.80
³⁵ Br	2.43	2	-6.42	-5.55	-6.37	-4.76	-3.91	-4.80
⁶⁶ Br	1.39	0	1.36	1.83	1.12	2.68	1.43	2.24
³⁵ Br	1.39	0	1.36	1.83	1.12	2.68	1.43	2.24
⁶⁸ Kr	1.46	0	1.34	1.83	1.13	2.65	1.41	2.22
³⁶ Kr	1.46	0	1.34	1.83	1.13	2.65	1.41	2.22
⁸¹ Mo	0.73	0	22.98	23.26	22.67	23.82	18.66	18.75
⁴² Mo	0.73	0	22.98	23.26	22.67	23.82	18.66	18.75
⁸⁵ Ru	1.13	0	13.67	14.08	13.76	14.66	11.19	11.59
⁴⁴ Ru	1.13	0	13.67	14.08	13.76	14.66	11.19	11.59
¹⁰⁸ Xe	1.01	0	26.64	27.07	26.37	27.47	20.87	20.87
⁵⁴ Xe	1.01	0	26.64	27.07	26.37	27.47	20.87	20.87

and the folded-Yukawa single-particle microscopic nuclear-structure model (FRDM) [49].

From Table I, it can be seen that my predictions agree with experimental data except for the $2p$ emitter ⁴⁸Ni. In the case of ⁴⁸Ni my prediction matches well with that of GLDM and GNL but shows a difference of order 5 with the experimental value. The reason for this difference is that the Q value used in present paper is $Q_{2p} = 1.950$ MeV (taken from Ref. [46]) which is 45% higher than the measured maximum value ($Q_{2p} = 1.350$ MeV [50]) and it is to be noted that a small error in Q value (1%) increases the penetrability by 40% which results in several orders of difference

in half-life. I would like to mention in my earlier work [35], I have used the experimental Q value and obtained a half-life value ($\log_{10}[T_{1/2}(s)] = -2.79$) which matches well with experimental value ($\log_{10}[T_{1/2}(s)] = -2.08$).

The good agreement between computed half-life values with experimental data and with other theoretical predictions, I extended my studies to 12 other nuclei for which $2p$ radioactivity is energetically possible with released energy, $Q_{2p} > 0$. The predicted half-life values using the CPPMDN and their comparison with other theoretical models and formulas are listed in Table II. In this table the first-third columns represent the nuclei, energy released Q_{2p} , and angular momentum

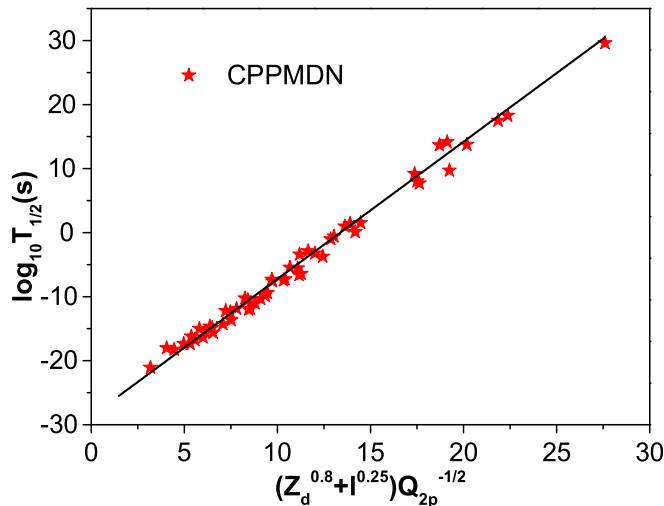


FIG. 1. The new Geiger Nuttall plot connecting $\log_{10}[T_{1/2}(s)]$ computed using the CPPMDN versus $[Z_d^{0.8} + \ell^{0.25}]Q_{2p}^{-1/2}$.

ℓ carried away by two emitted protons, respectively. The Q_{2p} values and angular momentum ℓ values are taken from Ref. [26]. The columns 4–11 represent the half-life values predicted by the model CPPMDN, ELDM [26], GLM [27], SEB [51], two-potential approach with SHF [52], GNL [30], and EF [29], respectively. From the table it is clear that overall, my prediction on half-life values match with other theoretical predictions.

Half-lives are also predicted for 39 nuclei whose $2p$ radioactivity are energetically possible, and their comparison with other theoretical models and/or formulas are given in Table III. The energy released Q_{2p} given in column 2 and the angular momentum ℓ given in column 3 are taken from Ref. [53]. The logarithm of half-lives predicted using the CPPMDN are given in column 4 and the UFM, GLDM, and ELDM values given, respectively, in the fifth–seventh columns are taken from Ref. [53]. Using the GNL of Liu *et al.* [30] and using the EF of Sreeja and Balasubramaniam [29], I have computed the logarithm of half-lives for these nuclei and are given in columns 8 and 9, respectively. In Table III one can see that the predictions on half-lives using the CPPMDN are matching with other theoretical predictions.

I have studied the new Geiger Nuttall plot connecting $\log_{10}[T_{1/2}(s)]$ computed using the CPPMDN versus $[Z_d^{0.8} + \ell^{0.25}]Q_{2p}^{-1/2}$ given in Fig. 1, and it is found to be linear which shows the reliability of my calculations. I have also studied the universal curve connecting $\log_{10}[T_{1/2}(s)]$ versus $-\ln P$

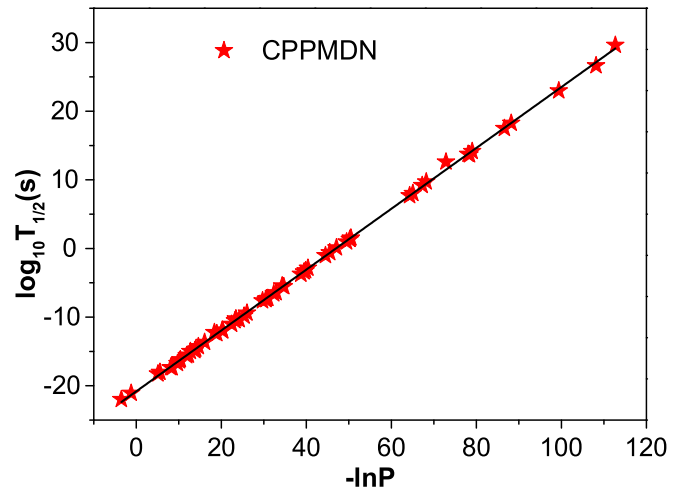


FIG. 2. The universal curve connecting $\log_{10}[T_{1/2}(s)]$ computed using the CPPMDN versus $-\ln P$.

given in Fig. 2 which also shows the linear nature with slope = 0.4433 and intercept = -20.81442 . It is to be noted that $2p$ radioactivity also obeys the universal curve connecting $\log_{10}[T_{1/2}(s)]$ versus $-\ln P$ as in the case of proton radioactivity [54], α , and cluster radioactivity [55,56].

IV. CONCLUSIONS

The $2p$ radioactivity from various nuclei ${}^6\text{Be}$, ${}^{12}\text{O}$, ${}^{16}\text{Ne}$, ${}^{19}\text{Mg}$, ${}^{45}\text{Fe}$, ${}^{48}\text{Ni}$, ${}^{54}\text{Zn}$, and ${}^{67}\text{Kr}$ have been studied using the CPPMDN, and the predicted half-life values are found comparable with the experimental data and with other models/formulas. The prediction on half-lives of 51 two-proton emitters, whose decays are energetically possible with released energy $Q_{2p} > 0$, which are not yet experimentally confirmed, will be a guide for future investigations. The new Geiger Nuttall plot connecting $\log_{10}[T_{1/2}(s)]$ computed using the CPPMDN with $[Z_d^{0.8} + \ell^{0.25}]Q_{2p}^{-1/2}$ and the universal curve connecting $\log_{10}[T_{1/2}(s)]$ with $-\ln P$ are found linear which emphasizes the reliability of my calculations. It is to be noted that as in the case of proton radioactivity, α , and cluster radioactivity, $2p$ radioactivity also obeys the universal curve.

ACKNOWLEDGMENTS

K.P.S. thanks the Council of Scientific and Industrial Research, Government of India, for the financial support under the scheme “Emeritus Scientist, CSIR”, Grant No. 21(1154)/22/EMR-II.

- [1] Y. B. Zel’dovich, *Sov. Phys. JETP* **11**, 812 (1960).
- [2] V. I. Goldansky, *Nucl. Phys.* **19**, 482 (1960).
- [3] V. I. Goldansky, *Nucl. Phys.* **27**, 648 (1961).
- [4] M. Pfützner, E. Badura, C. Bingham, B. Blank, M. Chartier, H. Geissel, J. Giovinazzo, L. V. Grigorenko, R. Grzywacz, and M. Hellström, *Eur. Phys. J. A* **14**, 279 (2002).
- [5] J. Giovinazzo, B. Blank, M. Chartier, S. Czajkowski, A. Fleury, M. J. Lopez Jimenez, M. S. Pravikoff, J.-C. Thomas, F. de

- Oliveira Santos, M. Lewitowicz, V. Maslov, M. Stanoiu, R. Grzywacz, M. Pfützner, C. Borcea, and B. A. Brown, *Phys. Rev. Lett.* **89**, 102501 (2002).
- [6] B. Blank, A. Bey, G. Cachel, C. Dossat, A. Fleury, J. Giovinazzo, I. Matea, N. Adimi, F. De Oliveira, I. Stefan, G. Georgiev, S. Grévy, J. C. Thomas, C. Borcea, D. Cortina, M. Caamano, M. Stanoiu, F. Aksouh, B. A. Brown, F. C. Barker, and W. A. Richter, *Phys. Rev. Lett.* **94**, 232501 (2005).

- [7] M. Pomorski, M. Pfützner, W. Dominik, R. Grzywacz, T. Baumann, J. S. Berryman, H. Czyrkowski, R. Dąbrowski, T. Ginter, J. Johnson, G. Kamiński, A. Kuźniak, N. Larson, S. N. Liddick, M. Madurga, C. Mazzocchi, S. Mianowski, K. Miernik, D. Miller, S. Paulauskas, J. Pereira, K. P. Rykaczewski, A. Stolz, and S. Suchyta, *Phys. Rev. C* **83**, 061303 (2011).
- [8] I. Mukha and K. Sümmerer, L. Acosta *et al.*, *Phys. Rev. Lett.* **99**, 182501 (2007).
- [9] T. Goigoux, P. Ascher, B. Blank, M. Gerbaux, J. Giovinazzo, S. Grévy, T. Kurtukian Nieto, C. Magron, P. Doornenbal, G. G. Kiss *et al.*, *Phys. Rev. Lett.* **117**, 162501 (2016).
- [10] W. Whaling, *Phys. Rev.* **150**, 836 (1966).
- [11] G. J. KeKelis, M. S. Zisman, D. K. Scott, R. Jahn, D. J. Vieira, J. Cerny, and F. Ajzenberg-Selove, *Phys. Rev. C* **17**, 1929 (1978).
- [12] P. Swan, *Rev. Mod. Phys.* **37**, 336 (1965).
- [13] B. D. Serot and J. D. Walecka, *Adv. Nucl. Phys.* **16**, 1, (1986).
- [14] J. Boguta and A. R. Bodmer, *Nucl. Phys. A.* **292**, 413, (1977).
- [15] Y. Sugahara and H. Toki, *Nucl. Phys. A.* **579**, 557, (1994).
- [16] P. Ring, *Prog. Part. Nucl. Phys.* **37**, 193, (1996).
- [17] H. L. Yadav, M. Kaushik, and H. Toki, *Int. J. Mod. Phys. E* **13**, 647, (2004).
- [18] G. Saxena, D. Singh, M. Kaushik, and S. Somorendro Singh, *Can. J. Phys.* **92**, 253, (2014).
- [19] M. Aggarwal, *Phys. Lett. B* **693**, 489, (2010).
- [20] M. Aggarwal, *Phys. Rev. C* **89**, 024325, (2014).
- [21] L. V. Grigorenko, R. C. Johnson, I. G. Mukha, I. J. Thompson, and M. V. Zhukov, *Phys. Rev. Lett.* **85**, 22 (2000).
- [22] L. V. Grigorenko, R. C. Johnson, I. G. Mukha, I. J. Thompson, and M. V. Zhukov, *Phys. Rev. C* **64**, 054002 (2001).
- [23] L. V. Grigorenko and M. V. Zhukov, *Phys. Rev. C* **68**, 054005 (2003).
- [24] L. V. Grigorenko and M. V. Zhukov, *Phys. Rev. C* **76**, 014008 (2007).
- [25] R. Álvarez-Rodríguez, H. O. U. Fynbo, A. S. Jensen, and E. Garrido, *Phys. Rev. Lett.* **100**, 192501 (2008).
- [26] M. Gonçalves, N. Teruyab, O. A. P. Tavares, and S. B. Duarte, *Phys. Lett. B* **774**, 14 (2017).
- [27] H.-M. Liu, X. Pan, Y.-T. Zou, J.-L. Chen, J.-H. Cheng, B. He, and X.-H. Li, *Chin. Phys. C* **45**, 044110 (2021).
- [28] J. P. Cui, Y. H. Gao, Y. Z. Wang, and J. Z. Gu, *Phys. Rev. C* **101**, 014301 (2020).
- [29] I. Sreeja and M. Balasubramaniam, *Eur. Phys. J. A* **55**, 33 (2019).
- [30] H.-M. Liu, Y.-T. Zou, X. Pan, J.-L. Chen, B. He, and X.-H. Li, *Chin. Phys. C* **45**, 024108 (2021).
- [31] K. P. Santhosh, J. G. Joseph, and S. Sahadevan, *Phys. Rev. C* **82**, 064605 (2010).
- [32] K. P. Santhosh and J. G. Joseph, *Phys. Rev. C* **86**, 024613 (2012).
- [33] K. P. Santhosh and A. Joseph, *Pramana* **58**, 611 (2002).
- [34] K. P. Santhosh, R. K. Biju, S. Sahadevan, and A. Joseph, *Phys. Scr.* **77**, 065201 (2008).
- [35] K. P. Santhosh, *Phys. Rev. C* **104**, 064613 (2021).
- [36] S. M. Wang and W. Nazarewicz, *Phys. Rev. Lett.* **120**, 212502 (2018).
- [37] N. Malhotra and R. K. Gupta, *Phys. Rev. C* **31**, 1179 (1985).
- [38] R. K. Gupta, M. Balasubramaniam, R. Kumar, N. Singh, M. Manhas, and W. Greiner, *J. Phys. G: Nucl. Part. Phys.* **31**, 631 (2005).
- [39] C. Y. Wong, *Phys. Rev. Lett.* **31**, 766 (1973).
- [40] A. J. Baltz and B. F. Bayman, *Phys. Rev. C* **26**, 1969 (1982).
- [41] Y. J. Shi and W. J. Swiatecki, *Nucl. Phys. A.* **464**, 205 (1987).
- [42] H. G. de Carvalho, J. B. Martins, and O. A. P. Tavares, *Phys. Rev. C* **34**, 2261 (1986).
- [43] J. Blocki, J. Randrup, W. J. Swiatecki, and C. F. Tsang, *Ann. Phys. (N.Y.)* **105**, 427 (1977).
- [44] V. Y. Denisov and A. A. Khudenko, *Phys. Rev. C* **79**, 054614 (2009).
- [45] K. N. Huang, M. Aoyagi, M. H. Chen, B. Crasemann, and H. Mark, *At. Data Nucl. Data Tables* **18**, 243 (1976).
- [46] Y. Wang, J. Cui, Y. Gao, and J. Gu, *Commun. Theor. Phys.* **73**, 075301(2021).
- [47] M. Wang, W. J. Huang, F. G. Kondev, G. Audi, and S. Naimi, *Chin. Phys. C* **45**, 030003 (2021).
- [48] H. Koura, T. Tachibana, M. Uno, and M. Yamada, *Prog. Theor. Phys.* **113**, 305 (2005).
- [49] P. Möller, A. J. Sierk, T. Ichikawa, and H. Sagawa, *At. Data Nucl. Data Tables* **109**, 1 (2016).
- [50] C. Dossat, A. Bey, B. Blank, G. Cachel, A. Fleury, J. Giovinazzo, I. Matea, F. de Oliveira Santos, G. Georgiev, S. Grévy, I. Stefan, J. C. Thomas, N. Adimi, C. Borcea, D. Cortina Gil, M. Caamano, M. Stanoiu, F. Aksouh, B. A. Brown, and L. V. Grigorenko, *Phys. Rev. C* **72**, 054315 (2005).
- [51] Y.-T. Zou, X. Pan, X.-H. Li, H.-M. Liu, X.-J. Wu, and B. He, *Chin. Phys. C* **45**, 104101 (2021).
- [52] X. Pan, Y.-T. Zou, H.-M. Liu, B. He, X.-H. Li, X.-J. Wu, and Z. Zhang, *Chin. Phys. C* **45**, 124104 (2021).
- [53] F. Xing, J. Cui, Y. Wang, and J. Gu, *Chin. Phys. C* **45**, 124105 (2021).
- [54] K. P. Santhosh and I. Sukumaran, *Phys. Rev. C* **96**, 034619 (2017).
- [55] D. N. Poenaru, R. A. Gherghescu, and W. Greiner, *Phys. Rev. C* **83**, 014601 (2011).
- [56] K. P. Santhosh and I. Sukumaran, *Braz. J. Phys.* **46**, 754 (2016).